

# Reconstruction-Diffusion: An Improved Maximum Entropy Reconstruction Algorithm Based on the Robust Anisotropic Diffusion

Harold I. A. Bustos<sup>1</sup> and Hae Yong Kim<sup>2</sup>

<sup>1</sup>*UFRN - Universidade Federal do Rio Grande do Norte, Centro de Tecnologia, Dept., Eng., Computação e Automação, Natal, RN – Brasil.  
harold@dca.ufrn.br*

<sup>2</sup>*USP Universidade de São Paulo, Escola Politecnica, Dept., de Sistemas Eletrônicos, São Paulo, SP - Brasil.  
hae@lps.usp.br*

## Abstract

Maximum entropy (MENT) is a well-known image reconstruction algorithm. If only a small amount of acquisition data is available, this algorithm converges to a noisy and blurry image. We propose an improvement to this algorithm that consists on applying alternately the MENT reconstruction and the robust anisotropic diffusion (RAD). We have tested this idea for the reconstruction from full-angle parallel acquisition data, but the idea can be applied to any data acquisition scenario. The new technique has yielded surprisingly clear images with sharp edges even using extremely small amount of projection data.

## 1. Introduction

Image reconstruction or tomography is the technique used to obtain the distribution of a non-directly observable medium from the projections. There are many tomography reconstruction techniques, for example, back-projection [1], Fourier transform [1], arithmetic reconstruction [1], maximum entropy (MENT) [2], extend-MENT [3], etc. In this paper, we are interested in tomography techniques that generate good reconstructed images even using small quantify of projection data.

In many practical situations, it is advantageous to minimize irradiation, in order to lessen the damage of the sample being irradiate or to speed up the data acquisition. The (MENT) algorithm is one of best-behaving techniques when only few data are available. However, even this method is appropriate only to enhance images with points-like features [4] We want to

develop a method that clearly reconstructs images with both points-like and regions-based features.

S. Baillet and L. Garnero [5] have recently proposed a MEG/EEG (Magnetoencephalography / Electroencephalography) tomography technique specially designed to enhance small discrete regions of active brain-cortex surrounded by regions of near-zero activity. The prior model used in this Bayesian approach is a non-convex potential function defined on the difference between each pair of neighboring pixel values. This potential function is a MRF (Markovian Random Field) that leads to a non-convex programming problem, using a Bayesian MAP (Maximum A Posteriori) approach. Baillet et al. have published recently other work on the same subject [6]. Furthermore, to deal with non-convexity and integer programming issues, some form of deterministic or stochastic annealing algorithms must be used. Computational costs can be very high for these methods. Therefore, this MAP approach leads to a very complex optimization task [7].

Anisotropic diffusion is a well-known technique used for filtering, edge finding and multi-scale image analysis. Recently, Black et al. have described the relationship between the anisotropic diffusion and the robust statistics, resulting a theoretically sound and improved technique named robust anisotropic diffusion (RAD) [8]. RAD has shown to be more efficient to smooth regions and detect edges than the classic anisotropic diffusion developed by Malik-Perona.

In this paper, we improve the extended-MENT algorithm using the RAD filtering. We call this new technique Reconstruction-Diffusion MENT (RD-

MENT). The main idea of the new algorithm is to intercalate, in each iteration step of the MENT, a RAD filtering. This idea is quite different from simply post-filtering an image generated by MENT. The MENT algorithm generates very noisy images caused by fluctuations of Lagrangian parameters, where even important edges are not clearly reconstructed [3]. In this scenario, no post-filtering can improve substantially the quality of reconstructed images. However, incorporating the RAD filtering into the extended-MENT algorithm, clear and sharp reconstructed images can be obtained, even using few projection data.

The extended-MENT is a convex functional with relation to posteriori output image  $f$  [3]. Incorporating the RAD priori leads to a more generalize extended-MENT Bayesian approach. The RAD prior model is obtained from descent gradient of Tukey's biweight robust statistic norm, which is a kind of non-Gaussian MRF (i.e., this norm is non-convex) [8, 9]. Therefore, the non-convexity of this norm must be appropriate to model both edges and smooth regions of images. Other attraction of the novel approach is that it guarantees to converge to a globally unique optimal solution, since it is based on the same extended-MENT cost functional which is convex and has a unique global minimum [3].

We describe our ideas for the image data acquisition scenario using parallel-beam and complete angle ( $180^\circ$ ). We have implemented and tested the proposed technique only for this situation. However, the ideas developed in this paper can be applied straightforwardly to any data acquisition circumstances: parallel-beam or fan-beam, full-angle or limited-angle, with missing or complete data. We have tested our algorithm using extremely small amount of projections data (i.e., our image reconstruction problem is severely ill-posed and under-determined).

## 2. Extended-MENT algorithm

Minerbo proposed the MENT algorithm [10] and subsequently various authors have proposed different improvements. For example, Dusassoy and Abdou [3] have introduced the extended-MENT that can process a priori information about the image to be reconstructed. If an approximation  $f^*$  of the image to be reconstructed  $f$  is known, this priori knowledge can be used to improve the reconstruction. The Lagrangian functional below represents the functional cost of the extended-MENT, subject to the restrictions of the synthetic phantom projections data:

$$L(f, \Lambda) = -\iint f(x, y) \log \left[ \frac{f(x, y)}{ef^*(x, y)} \right] dx dy - \sum_{j=1}^J \sum_{n=1}^N \Lambda_{j,n} \left[ h_{j,n} - \iint f(x, y) \chi_{j,n}(x, y) dx dy \right] \quad (1)$$

where:

- $e$  is the Napierian base (2.71828...).
- $h_{j,n}$  is the intensity of  $n$ -th parallel ray of the projection  $j$ .
- $\Lambda_{j,n}$  is the Lagrange parameter associated with the stripe  $(j, n)$ . If complete data were available, this coefficient would always be one.
- $\chi_{j,n}$  is the indicator function of the stripe  $(j, n)$ . This function is 1 inside the region covered by the stripe  $(j, n)$  and 0 outside.
- $f^*(x, y)$  is the prior model of the object  $f(x, y)$
- When no prior information is available,  $f^*(x, y)$  can be set to  $e^{-1}$ . In this case, the extended-MENT becomes the original Minerbo's MENT.

Optimization of equation (1), via Frechet derivate, allows us to find the solution of the reconstruction problem:

$$f^{(i)}(x, y) = f^*(x, y) \prod_{j=1}^J \sum_{n=1}^N F_{j,n}^{(i)} \chi_{j,n}(x, y), 1 \leq i \leq \zeta \quad (2)$$

where  $F_{j,n}$  is the matrix of dual Lagrange parameters associated with the stripe  $(j, n)$ . These parameters are obtained by the following iterative system:

$$F_{j,n}^{(i)} = \begin{cases} z h_{j,n}, i = 0 \\ \frac{h_{j,n}}{\iint f^*(x, y) \prod_{\substack{k=1 \\ k \neq j}}^J \sum_{n=1}^N [F_{k,n}^{(i-1)} \chi_{k,n}(x, y)] \chi_{j,n}(x, y) dx dy}, 1 \leq i \leq \zeta \end{cases} \quad (3)$$

where  $z$  is the whole width of the projection  $j$ . After computing  $F_{j,n}^{(i)}$ , they must be inserted in (2) to find the reconstructed image  $f^{(i)}(x, y)$ .

The sensitivity of this algorithm, as is defined in [3], is proportional to the images values  $f(x, y)$ . Practically, this means that larger values of  $f$  will vary more than small ones when parameter  $F_{j,n}$  changes slightly. Thus, it is expected that the reconstructed images will contain more noise in the higher density sections. Consequently, the noise will not be of the additive Gaus-

sian kind. This is an important characteristic of the MENT solution that will be reflected in the reconstructed images.

### 3. Robust anisotropic diffusion

Black et al. [8] have proposed the robust anisotropic diffusion (RAD). It assumes that the input is a piecewise smooth image corrupted by zero-mean additive Gaussian noise with small standard deviation. The goal is to estimate the original image from the noisy data. Black et al. have used the robust statistics to solve this problem. They compute an image  $I$  that satisfies the following optimization criterion:

$$\min_I \sum_{s \in I} \sum_{p \in \eta_s} \rho(I_p - I_s, \sigma) \quad (4)$$

where  $I_s$  is the value of image  $I$  at pixel  $s$ ,  $\eta_s$  is the spatial neighborhood of pixel  $s$ ,  $\rho(\cdot)$  is a robust error norm and  $\sigma$  is a scale parameter that must be adjusted to filter noise and preserve edges. Black et al. solved equation (4) by gradient descent:

$$I_s^{(t+1)} = I_s^{(t)} + \frac{\lambda}{|\eta_s|} \sum_{p \in \eta_s} g\left(\left|\nabla I_{s,p}^{(t)}\right|\right) \nabla I_{s,p}^{(t)} \quad (5)$$

where  $g(x) = \rho'(x)/x$ , the constant  $\lambda \in \mathfrak{R}^+$  is a scalar that determines the rate of diffusion, and  $\nabla I_{s,p}^{(t)}$  represents the gradient at pixel  $s$  in relation to the neighbor pixel  $p$ .

Black et al. have chosen Tukey's biweight as the error norm and it has shown to be an excellent edge detector (better than Perona-Malik's classic edge detector [11]):

$$g(\nabla I, \sigma) = \begin{cases} \frac{1}{2} \left[ 1 - \left( \frac{|\nabla I|}{\sigma} \right)^2 \right]^2, & \text{if } |\nabla I| \leq \sigma \\ 0, & \text{otherwise} \end{cases} \quad (6)$$

Let us suppose that the image  $I$  consists of regions with smooth gray-scale variation. Intuitively, RAD performs intra-region neighborhood averaging and avoids performing inter-region averaging. So, this process attenuates noise while keeping sharp inter-region edges.

Theoretically, the gradient descent process can converge to a local minimum because the  $\rho(\cdot)$  norm is non-convex. However, in practice, RAD has shown to yield excellent solutions. Moreover, it seems that similar processes using convex norms converge to a trivial constant grayscale images (that is completely useless in practice).

### 4. The proposed algorithm: RD-MENT

Let us suppose that the image  $f$  to be reconstructed is piecewise smooth. As we remarked before, in scarce-data condition, the extended-MENT algorithm will reconstruct a noisy image contaminated with artifacts. RAD is an excellent estimator of the original image  $f$  from its corrupted version. However, using it as a post-filtering process, only a slight enhancement can be obtained. Our idea is to use this slightly enhanced image as a priori knowledge  $f^*$  of the extended-MENT algorithm. This will yield better-reconstructed image. This improved image can be further enhanced by the RAD and used as new a priori knowledge of the extended-MENT. And so on.

Initially, we apply the extended-MENT algorithm, iterating equation (3)  $\zeta$  times. Using (2), the reconstructed image  $f^{(\zeta)}$  is obtained. This image is filtered by RAD, iterating (5) one or more times. The filtered image is used as a priori image  $f^*$  in extended-MENT (3) to obtain a new reconstructed image. This image is filtered again by RAD, and so on, until the difference between the two consecutive images are below some threshold.

### 5. Experimental results

To show the effectiveness of the proposed technique, we executed some experiments. The simulated test object is a cylinder with diameter 100 and density 5, immersed in background medium with density 0 (figure 1a). This cylinder contains five inner off-centered cylinders with varied diameters and densities. Experiments consisted on reconstructing  $100 \times 100$  images from only 6 parallel projections distributed over complete angle ( $180^\circ$ ), each projection with 100 irradiated rays.

Image 1b was obtained by the original extended-MENT, iterating equation (3) 10 times. This image was filtered by RAD ( $\sigma=32$ , 100 iterations), generating image 1c. It was used as the initial estimate of the RD-MENT. Reconstruction-diffusion (that is, one execution of (3) followed by one execution of (5)) was iterated 9 times (with  $\sigma=32$ ), generating image 1d. Clearly, the new algorithm generates a better image. The mean absolute differences between the ideal image 1a and images 1b, 1c, 1d are respectively 12.7%, 12.8%, and 7.5%.

Let us define the reconstructed projections  $h_{j,n}^{(i)}$ , computed from the reconstructed image at  $i$ -th iteration  $f^{(i)}$ , as:

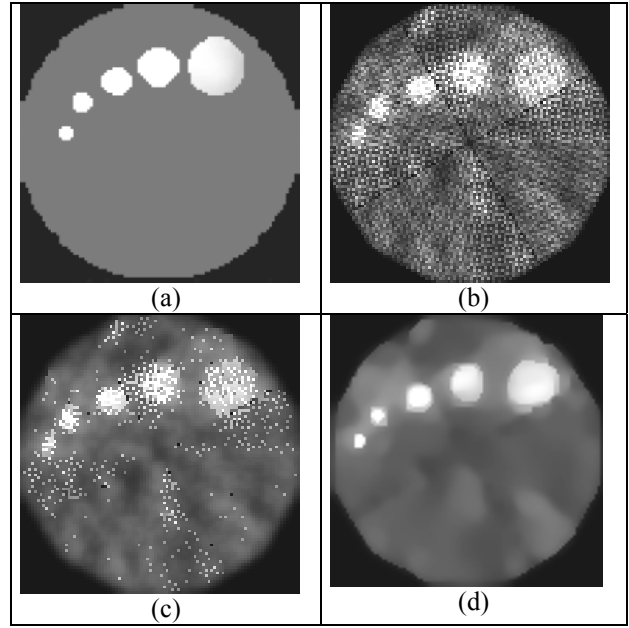
$$h_{j,n}^{(i)} = \iint f^{(i)}(x,y)\chi_{j,n}(x,y) dx dy \quad (7)$$

Let us define the Euclidean norm  $k^{(i)}$  between the original projections  $h_{j,n}$  and the projections computed from reconstructed image  $h_{j,n}^{(i)}$  as:

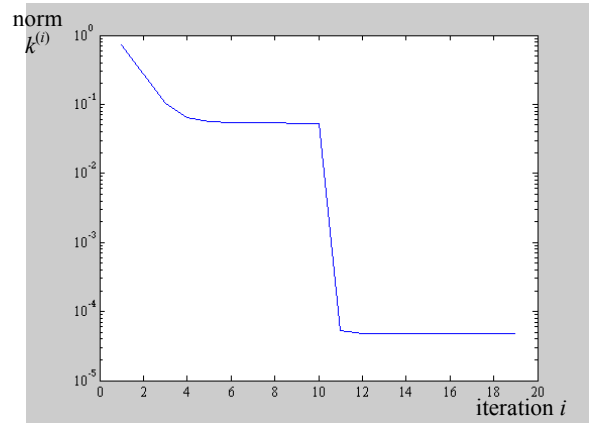
$$k^{(i)} = \sqrt{\sum_{j=1}^J \sum_{n=1}^N (h_{j,n}^{(i)} - h_{j,n})^2} \quad (8)$$

Figure 2 shows Euclidean norms  $k^{(i)}$  of different iteration phases of the reconstruction. The first 10 iterations correspond to the original extended-MENT and the last 9 iterations to the proposed RD-MENT. Clearly, the Euclidean norm converges faster using the proposed algorithm. The scale parameter  $\sigma=32$  was chosen to maximize convergence of the Euclidean norm. After the iteration 12, this norm becomes almost constant. This seems to show that RD-MENT solution minimizes the Euclidean norm.

Another artificially generated phantom is depicted in figure 3a. Six parallel projections distributed over  $180^\circ$  with 100 rays per projection (600 total rays) were irradiated. The original extended-MENT was executed over these data, generating image 3b. Image 3b was filtered by RAD ( $\sigma=50$  and 70 iterations), generating image 3c. Clearly, post-filtering cannot generate a clear reconstructed image. Image 3c was used as the initial estimate of the image to-be-reconstructed by the RD-MENT. This algorithm was iterated 70 times using scale parameter  $\sigma=50$ , generating image 3d. Clearly, the proposed algorithm generates the best image. All images have resolution  $100 \times 100$  pixels. The mean absolute differences between the ideal image 3a and images 3b, 3c and 3d are respectively 14.89%, 15.22% and 8.15%. Using the well-known filtered back-projection, the poor-quality image 3e was obtained. This poor result was caused by under-sampling of acquisition data. In this scenario, filtered back-projection yield artifacts on the output image since sampling frequencies are below the Nyquist frequency [1] (see figure 3e).



**Fig. 1:** (a) Synthetic phantom; (b) original extended-MENT; (c) image 1b filtered by RAD; (d) the proposed RD-MENT.



**Fig. 2:** Euclidean norm  $k^{(i)}$  of the differences between the original projections and the projections computed from reconstructed images at  $i$ -th iteration. The first 10 iterations correspond to the original extended-MENT and the last 9 iterations to the proposed RD-MENT.

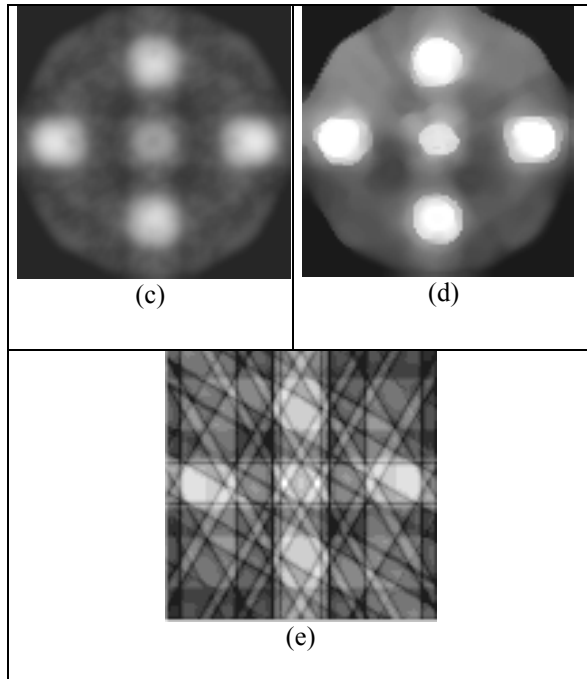


**Fig. 3:** (a) Synthetic phantom; (b) original extended-MENT; (c) image 3b filtered by RAD; (d) the proposed RD-MENT; (e) image reconstructed by the filtered back-projection.

## 6. Conclusion

In this paper, we have proposed an improvement to the classic extended-MENT reconstruction algorithm, named RD-MENT. The new technique is based on the robust anisotropic diffusion (RAD). The RAD filtering is incorporated into the extended-MENT algorithm. The new algorithm generated clear and sharp reconstructed images, even using very small amount of projection data. Experimental data demonstrate the effectiveness of the proposed technique.

## 7. Acknowledgements

Authors would like to express their gratitude to CNPq for the partial financial support of this work under grants 303541/2003-2, 305065/2003-3 and 475155/2004-1 and to FAPESP under grant 2003/13752-9.

## 8. References

- [1] A. K. Jain, *Fundamentals of Digital Image Processing*, Prentice Hall, 1989.
- [2] M. L. Reis and N. C. Roberty, "Maximum-Entropy Algorithms for Image-Reconstruction from Projections," *Inverse Problems*, vol. 8, no. 4, 1992, pp. 623-644.

- [3] N. J. Dusasoy and I. E. Abdou, "The Extended MENT Algorithm: A Maximum Entropy Type Algorithm Using Prior Knowledge for Computerized Tomography," *IEEE T. Signal Processing*, vol. 39, no. 5, May 1991, pp. 1164-1180.
- [4] B. Borden, "Maximum Entropy Regularization in Inverse Synthetic Aperture Radar Imagery," *IEEE Trans. Signal Processing*, vol. 40, no. 4, Apr. 1992, pp. 969-973.
- [5] S. Baillet and L. Garnero, "A Bayesian Approach to Introducing Anatomic-Functional Priors in the EEG/MEG Inverse Problem," *IEEE Trans. Biomed. Eng.*, vol. 44, 1997, pp. 374-385.
- [6] S. Baillet, J. C. Mosher, and R. M. Leahy, "Electromagnetic Brain Mapping," *IEEE Signal Processing Magazine*, Nov. 2001, pp. 14-30.
- [7] S. Geman and D. Geman, "Stochastic relaxation, Gibbs distribution and the Bayesian restoration of images," *IEEE Trans. Pattern Anal. Machine Intell.*, vol. PAMI-6, Nov. 1984, pp. 721-741.
- [8] M. J. Black, G. Sapiro, D. H. Marimont, and D. Heeger, "Robust Anisotropic Diffusion," *IEEE T. Image Processing*, vol. 7, no. 3, March 1998, pp. 421-432.
- [9] C. Bouman and K. Sauer, "A Generalized Gaussian Image Model for Edge-Preserving MAP Estimation," *IEEE Transactions on Image Processing*, vol. 2, no. 3, July 1993, pp. 296-310.
- [10] G. Minerbo, "MENT: A Maximum Entropy Algorithm for Reconstructing a Source from Projection Data," *Comput. Graph. Image Processing*, vol. 10, 1979, pp. 48-68.
- [11] P. Perona and J. Malik, "Scale-Space and Edge Detection Using Anisotropic Diffusion," *IEEE Trans. Pattern Anal. Machine Intell.*, vol. 12, no. 7 pp. 629-639, July 1990.